Journal of Inflammation Research

Dovepress
open access to scientific and medical research

Open Access Full Text Article

ORIGINAL RESEARCH

Shenfu Injection Mediated NLRP3/Caspase 1 Through (R)-Norcoclaurinee Alleviates Sepsis-Induced Cognitive Dysfunction

Xinqiang Liu[1,*], Hongguang Ding[2,*], Miner Chen[1,*], Xusheng Li[2], Yan Xiao[1], Yongli Han[1], Hongke Zeng[1]

[1]Department of Intensive Care Medicine, Guangdong Provincial People's Hospital (Guangdong Academy of Medical Sciences), Southern Medical University, Guangzhou, 510800, People's Republic of China; [2]Department of Emergency Medicine, Guangdong Provincial People's Hospital (Guangdong Academy of Medical Sciences), Southern Medical University, Guangzhou, 510800, People's Republic of China

*These authors contributed equally to this work

Correspondence: Hongke Zeng, Department of Intensive Care Medicine, Guangdong Provincial People's Hospital (Guangdong Academy of Medical Sciences), Southern Medical University, No. 106, Zhongshan 2nd Road, Guangzhou, People's Republic of China, 510080, Tel/Fax +8602083827812-60810, Email zenghongke@gdph.org.cn

Background: Shenfu injection (SF) has demonstrated its potential to enhance cellular immunity and induce clinical regression in patients suffering from sepsis or infectious shock. However, the therapeutic effect of SF on sepsis-induced cognitive dysfunction (SAE) and the mechanisms involved are still unclear. We aimed to investigate the mechanism of SF in mice with SAE.

Methods: Sepsis was constructed by caecal ligation and puncture. Mice were injected intraperitoneally with SF or NLRP3 inhibitor. The hippocampus injury of brain tissues was evaluated, and the levels of inflammatory cytokines (IL-1β, IL-18) and NLRP3 and Caspase 1 were measured. The active ingredients of SF were analyzed using network pharmacology, and molecular docking of the active ingredients of SF with NLRP3 and Caspase 1 was performed. BV-2 cells were treated with LPS or norcoclaurine. CCK-8 detected the cell viability, and the levels of inflammatory cytokines and NLRP3 and Caspase 1 were measured.

Results: SF and NLRP3 inhibitor increased survival rate and the number of crossing the platform and decreased the escape latency time of sepsis mice. Moreover, SF and NLRP3 inhibitor improved neuronal damage and apoptosis in hippocampus of sepsis mice. In addition, SF and NLRP3 inhibitor reduced the levels of inflammatory cytokines, as well as inflammasomes in sepsis mice. There were 43 active ingredients in SF. Among them, 22 were Renshen and 21 were Fuzi. Renshen and Fuzi, the main active components of SF, form a complex regulatory network with NLRP3 and Caspase 1. (R)-norcoclaurine was most closely bound to NLRP3 with binding energy of −7.2 kJ·mol^{-1}, ignavine was most closely bound to Caspase 1 with binding energy of −8.3 kJ·mol^{-1}. Norcoclaurine increased the cell viability and decreased inflammation and pyroptosis.

Conclusion: SF regulated NLRP3/Caspase 1 through (R)-norcoclaurinee to prevent SAE.

Keywords: shenfu injection, NLRP3, caspase 1, pyroptosis, sepsis-associated encephalopathy

Introduction

Sepsis-associated encephalopathy (SAE) is a serious and frequently encountered complication of sepsis,[1] which could lead to acute cognitive and consciousness disorders.[2] SAE is linked to increased mortality, decreased quality of life, and long-term neurological complications, ranging from 9% to 76% in patients with SAE diagnosed with sepsis progression.[3] The pathogenesis of SAE involves neuroinflammatory response, neurotransmitter dysfunction, destruction of blood-brain barrier, and abnormal blood flow regulation.[4] At present, the treatment of SAE is mainly symptomatic. Lack of specific treatment plans and insufficient understanding of the underlying mechanism of the disease are the reasons for poor prognosis of sepsis patients.[5] Therefore, it is of great significance to explore the treatment and underlying mechanisms of

Received: 3 June 2024
Accepted: 27 September 2024
Published: 14 October 2024

SAE, as well as implement preventive measures to reduce its occurrence and lower the incidence rate, so as to improve the prognosis of sepsis patients.

Herbal injections contain a large number of hydrophilic components, and an in-depth understanding of their chemical composition, both qualitatively and quantitatively, is important to ensure the safety of their clinical use.[6] As a novel and promising option for the treatment of sepsis, herbal injections are widely used in China.[7] Shenfu injection (SF) derived from traditional Chinese medicine (TCM), which prepared from red ginseng and processed aconite root, is widely used in China for sepsis and cardiovascular diseases.[8,9] SF has various anti-inflammatory, anti-apoptotic, antioxidant and innate immunomodulatory effects.[10–12] These pharmacological effects may be attributed to the active constituents of the compound, which mainly consists of ginsenosides and aconite alkaloids.[6] Study has shown that SF could reduce cardiac dysfunction and inhibit apoptosis in septic mice.[13] In addition, SF has demonstrated its potential to enhance cellular immunity and induce clinical regression in patients suffering from sepsis or infectious shock.[14] However, the therapeutic effect of SF on SAE and the mechanisms involved are still unclear.

Pyroptosis is a form of programmed cell death triggered by the activation of specific inflammatory cysteinases through the inflammasome complex, including nucleotide binding oligomerization domain-like receptor family pyrin domain protein 3 (NLRP3).[15] The main function of NLRP3 inflammasomes is to promote the secretion of interleukin (IL)-1β and IL-18, as well as Caspase 1-mediated pyroptosis.[16] Indeed, research has demonstrated the involvement of NLRP3 inflammasomes in the pathogenesis and advancement of immune inflammatory conditions such as sepsis.[17] Energy metabolism and respiratory dysfunction during sepsis can lead to the generation of reactive oxygen species, which not only induce oxidative damage to tissues and organelles but also directly or indirectly activate NLRP3 inflammasomes. The activation of NLRP3 inflammasomes, in turn, enhances the inflammatory response, triggers apoptosis in immune cells, and worsens the progression of sepsis.[18] In addition, NLRP3/Caspase 1 pathway-mediated pyroptosis has been found to contribute to cognitive impairments in a mouse model of SAE.[19] Zhou et al reported that Ginsenoside Rg1 reduced blood-brain barrier damage by inhibiting NLRP3/Caspase 1/gasdermin D (GSDMD) mediated classic pathway of pyroptosis, thereby improving SAE and thus playing a brain protective role.[20] However, it is unclear whether SF improves SAE through NLRP3/Caspase 1-mediated pyroptosis.

Based on the above background, we intend to detect the regulatory effect of SF on NLRP3/Caspase 1 mediated pyroptosis, and explore the potential mechanism of SF in treating SAE. Our study offers a novel strategy for the prevention and treatment of clinical SAE, while also establishing a molecular foundation for the utilization of TCM in SAE treatment.

Materials and Methods

Animals

Forty male C57BL/6 mice aged 6–8 weeks and weighing 20–25 g were obtained from Guangzhou Ruige Biotechnology Co., Ltd (Guangzhou, China). The mice were housed in a controlled environment with a 12-hour light-dark cycle, maintained at a room temperature of 22–24°C, and humidity levels ranging from 30% to 70%. They were given free food and water before the experiment. The mice were randomly divided into 4 groups: Control, caecal ligation and puncture (CLP), CLP + SF, CLP + NLRP3 inhibitor, with 10 mice in each group. One hour before operation, mice in CLP +SF group were injected intraperitoneally with SF (10 mL/kg, CR SANJIU, Henan, China).[13,21] Mice in CLP + NLRP3 inhibitor group were injected intraperitoneally with NLRP3 inhibitor (70 mg/kg).[22] Mice in Control and CLP groups were injected with normal saline. One hour later, a mouse model of sepsis was constructed by CLP.[23–25] In the Control group, only laparotomy was performed, denoted as day zero. The survival rate of mice was analyzed from day one to the fifth day after operation. Morris water maze (MWM) was performed from day one to the fourth day postoperatively to record the escape latency time. On the 5th day, water maze without platform detection was performed. After anesthesia with 2% isoflurane, the eyeballs were removed to obtain blood for serum separation and whole brain tissue (separated by coronal transection) was taken. The mice were euthanized ethically when they were near death. Mice are euthanized by exposure to carbon dioxide. All animal experiments have been approved by ethics committee of Guangdong Provincial People's Hospital (approval number KY–H–2022-004-03), and performed in according with the IACUC Handbook, Third Edition.

MWM

MWM test (one min/time) was performed on mice from day one to the fourth day after surgery to record the escape latency time to evaluate their cognitive function.[26,27] During the acquisition phase, the mice were introduced into the pool from four different entry points facing the pool wall. The time it took for each mouse to enter the water, find, and stand on the submerged hidden platform was recorded as the escape latency, denoted in s. After the mice successfully located the platform, they were permitted to remain on it for 10s. In cases where the mice were unable to locate the platform within 60s, they were gently guided to the platform from the water, where they stayed for 10s before the next training. Each mouse was placed into the pool from each of the four entry points as one training session, with a 30s interval between sessions.

Hematoxylin-Eosin (HE) Staining

To detect pathological changes in the hippocampal region (DG and CA3) of the brain tissues, HE staining was employed. Mouse brain tissues were taken and fixed in tissue fixative (G1101, Servicebio, Wuhan, China). The tissue slices were subjected to baking at 60°C for 1–2 h, followed by dewaxing and rinsing in distilled water. Hematoxylin (G1003, Servicebio) was then applied to stain the slices for 5–10 min, after which they were rinsed again with distilled water and subjected to a brief phosphate buffer saline (PBS) rinse to restore a blue color. Eosin was used to stain for 3–5 min. Gradient alcohol (95–100%) dehydration was performed for 5 min in each stage. After removal, the slices were immersed in xylene (10023418, Sinopharm Chemical Reagent Co., Ltd, Shanghai, China) two times for 10 min each. Subsequently, the slices were sealed with neutral gum (10004160, Sinopharm Chemical Reagent Co., Ltd) and examined using a fluorescence microscope (BA210T, Motic, Xiamen, China).

TdT Mediated dUTP Nick End Labeling (Tunel)

Apoptosis in the hippocampal region (DG and CA3) of brain tissues was detected using Tunel kit (G1502, Servicebio). Hippocampal tissues were sliced and baked at 60°C for 30–60 min, and the slices were deparaffinised to water. 100 μL of proteinase K (G1205, Servicebio) was added dropwise to each sample and incubated at 37°C for 20 min. Following this, the slices were rinsed three times in PBS, with each rinse lasting for 5 min. Appropriate amount of membrane-breaking solution (G1204, servicebio) was added dropwise to the tissues, and the tissues were fully infiltrated and processed at room temperature for 20 min. The samples were washed with PBS. Then, for each sample, 100 μL of 1 × Equilibration Buffer was added dropwise to cover the specific area to be examined, followed by incubation at room temperature for 10–30 min. TdT enzyme incubation buffer was prepared, and excess 1 × Equilibration Buffer (100 μL) was carefully removed from the equilibrated area using absorbent paper. Subsequently, 50 μL of TdT enzyme incubation buffer was added to the tissue samples being examined. TdT enzyme incubation buffer was added to the tested tissues, followed by incubation at 37°C for 60 min in the absence of light. The nuclei were then rinsed three times with PBS for 5 min each. Afterward, DAPI (G1012, servicebio) was used to stain the nuclei at 37°C for 10 min. Finally, the slices were sealed with neutral gum and observed under a fluorescence microscope.

Enzyme-Linked Immunosorbent Assay (ELISA)

The levels of IL-1β and IL-18 in serum and brain tissue of mice were measured. IL-1β (RX203063M, Risen Bio, Quanzhou, China) and IL-18 (RX203064M, Risen Bio) kits were used to detect inflammatory cytokines IL-1β and IL-18 according to the instructions.

Western Blot

Western blot was utilized to quantify NLRP3 and Caspase 1 expressions in brain tissues, or Caspase 1, NLRP3, IL-18, and IL-1β expression in BV-2 cells. Total proteins were extracted from brain tissues or cells using radioimmunoprecipitation assay (P0013B, Beyotime, Shanghai, China) following the provided instructions. Protein quantification for each group of samples was performed using the bicinchoninic acid (BCA) Kit (BL521A, Biosharp, Hefei, China). Sodium dodecyl sulfate, sodium salt polyacrylamide gel electrophoresis loading buffer (MB2479, meilunbio, Dalian, China) was mixed with the samples, and the mixtures were heated in a boiling water bath at 100°C for 5 min. The

proteins were then electrophoretically transferred onto a polyvinylidene fluoride membrane and blocked with a 5% skimmed milk solution at room temperature for 90 min. The samples were incubated with primary antibodies against NLRP3 (13158s, Cell Signaling Technology, Danvers, MA, USA), Caspase 1 (22,915-1-AP, Proteintech, Wuhan, China), IL-18 (A1115, ABCLONAL, Wuhan, China), IL-1β (A1112, ABCLONAL), GAPDH (60004-1-Ig, Proteintech) and β-actin (66009-1-Ig, Proteintech) overnight at 4°C. Membrane washed with TBST (three times at room temperature). Then, membrane incubated with the secondary antibodies Goat anti-Rabbit IgG-HRP (BL003A, Biosharp) or Goat anti-Mouse IgG-HRP (BL001A, Biosharp). ECL chemiluminescent substrate (K-12045-D50, advansta, Beijing, China) was used for visualization of proteins. Protein bands were analyzed by imaging with software (Chemiscope6100, CLINX, Shanghai, China). GAPDH and β-actin was used as an internal reference.

Immunofluorescence (IF)

IF was used to detect NLRP3/Caspase 1 and NeuN expression in the hippocampus of brain tissues. Slices were baked at 60°C for 12 h and deparaffinised to water. They were then washed sequentially in 100%, 100%, 95%, 85%, and 75% ethanol for 5 min at each level, and rinsed in distilled water for 5 min. Slices were heated to repair antigens, and endogenous enzymes were inactivated by adding 3% H_2O_2 for 10 min, and the slices were blocked with 5% bovine serum albumin (BS114-100g, Biosharp) for 60 min. Appropriately diluted primary antibodies against NLRP3 (13158s, CST), Caspase 1 (22,915-1-AP, Proteintech), and NeuN (26975-1-AP, Proteintech) were incubated at 4°C overnight. Subsequently, secondary antibody (RC0086-23, Recordbio Biological Technology, Shanghai, China) was incubated at 37°C for 90 min, and the nuclei were stained with DAPI at 37°C for 10 min. Antifade mounting medium (G1401, servicebio) was used to seal the slices, which were then visualized under fluorescence microscope.

Acquisition of Active Ingredients for SF

All components of Renshen and Fuzi in SF were obtained through the Traditional Chinese Medicine systems pharmacology database and analysis platform (TCMSP, https://tcmspw.com /tcmsp.php). Compounds were screened according to ADME parameters (drug-likeness (DL) ≥ 0.18 and oral bioavailability (OB) ≥ 30%).

The Molecular Docking Analysis of the Active Ingredients of SF and the Targets NLRP3 and Caspase 1

The mol2 structure files of SF active ingredients were downloaded from TCMSP database and the PDB files of NLRP3 and Caspase 1 were obtained from RCSB PDB (https://www.rcsb.org/) database. Receptor protein was optimized by AutoDockTools and converted into pdbqt format. AutoDock Vina 1.1.2 was utilized to conduct molecular docking between the receptor protein and the ligand small molecule, resulting in the calculation of the binding energy score. If the binding energy was < 0, it indicated that the ligand molecule could bind spontaneously to the receptor protein. Furthermore, if the binding energy was ≤ −5.0 $kJ \cdot mol^{-1}$, it indicated a strong binding property. Typically, a lower binding energy signifies a stronger binding effect between the two molecules. The top three molecules with the closest binding degree to each target were selected to showed the molecular docking model using Discovery Studio 2019 software.

BV-2 Cells Culture and Cell Viability

BV-2 cells (337749, BNCC, Henan, China) were cultured in DMEM-H supplemented with 10% FBS at 37°C in a 5% CO_2 incubator. Cells were confirmed by STR method. To detect the cell viability, BV-2 cells (3000 cells/well in 96-well plate) were divided four groups, Control group (normal cultivation), lipopolysaccharide (LPS) group (treated with LPS), LPS + DMSO group (treated with LPS and dimethyl sulfoxide (DMSO)), and LPS + norcoclaurine (treated with 200 ng/mL LPS (L2880, Sigma, St. Louis, MO, USA) and norcoclaurine (HY-N2037A, Med Chem Express, Shanghai, China). After treatment for 24 h, 10% Cell Counting Kit-8 (CCK-8) regent (BS350B, Biosharp) was added to each well and continue to cultivate for 2 h. The values were obtained at the 450 nm. Relative viability was calculated compared to the Control group.

Statistical Analysis

Statistical analysis was conducted using GraphPad Prism 8.0 software GraphPad Software Inc., San Diego, CA, USA). Measurement data were presented as mean ± standard deviation. Comparisons between multiple groups were performed using One-way analysis of variance. A significance level of $P < 0.05$ was considered statistically significant.

Results

Comparison of Survival and Mortality and Behavioral Detection in Mice

First, we applied CLP to mice to assess survival and mortality. Compared to the Control group, the survival rate of mice in CLP group significantly decreased over time (from day one to the fifth day), and the end point of death was 5 mice. With the use of SF and NLRP3 inhibitor, the survival rate of mice was improved, and the end point of death was 4 and 3 mice, respectively (Figure 1A). Base on the records of weight, compared to the Control group, the weight of the other

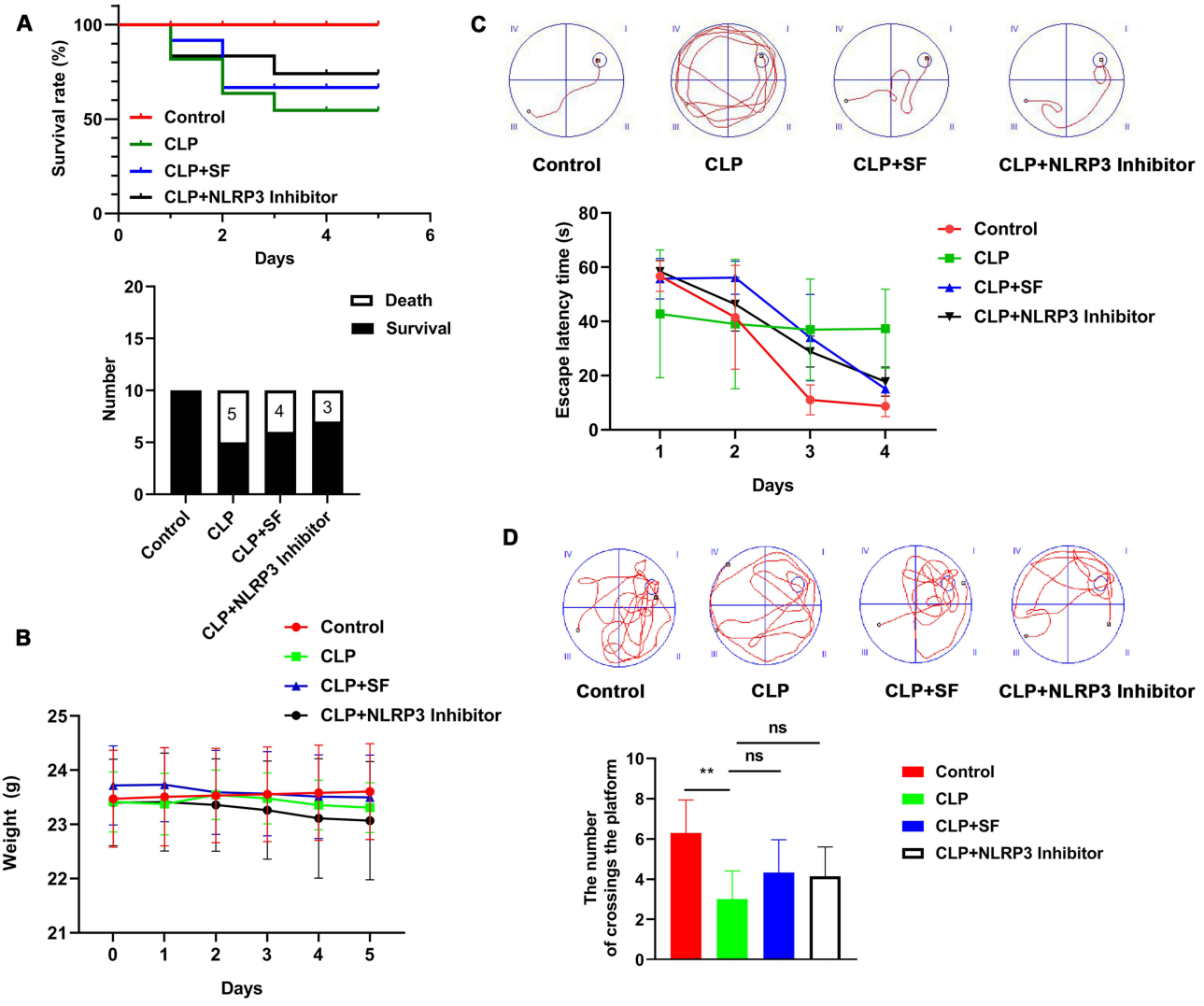

Figure 1 Comparison of survival and mortality and behavioral detection in mice. (**A**) Percentage comparison of survival and number of endpoint deaths in mice from day one to the fifth day. n=10 mice/group. (**B**) The weight of mice from day one to the fifth day. (**C**) Morris water maze recordings of the escape latency time. The upper panel shows the third quadrant experimental graph on the fourth day. The lower graph shows the graph of the escape latency time on from day one to the fourth day. I, II, III, and IV correspond to quadrant 1, 2, 3, and 4, respectively. The black circle is the location information point at the beginning of the mouse experiment, the black square is the location information point at the end of the mouse experiment, and the blue circular area is the hidden underwater platform position. (**D**) Water maze behavioral tested the number of crossings the platform. The upper panel shows the third quadrant experimental graph on the fifth day. The lower graph shows the the inter group analysis. I, II, III, and IV correspond to quadrant 1, 2, 3, and 4, respectively. The black circle is the location information point at the beginning of the mouse experiment, the black square is the location information point at the end of the mouse experiment, and the blue circular area is the hidden underwater platform position. **P < 0.01; ns, no significant.
Abbreviations: CLP, caecal ligation and puncture; SF, shenfu injection.

three groups of mice slightly decreased on day zero and the first day, but there was no statistically significant difference (Figure 1B). From the activity trace diagram of the MWM of mice on the fourth day, the activity trace of mice in CLP group was much higher than that in CLP + SF and CLP + NLRP3 inhibitor groups. Then, the escape latency time of mice was analyzed. Compared to Control group, the escape latency time of mice in the CLP group significantly increased starting from the third day. However, the escape latency time of mice was reduced after treatment with SF and NLRP3 inhibitor (Figure 1C). In addition, water maze without platform detection on the fifth day showed that the spatial memory of CLP group mice was worse than the other three groups, with fewer crossings of the original platform compared to the other three groups (Figure 1D).

Pathological Analysis of the Hippocampal Region (DG and CA3) of Mouse Brain Tissue

Next, we analyzed the pathology of the hippocampal region of brain tissueS. HE staining showed that compared to Control group, neuronal damage in the hippocampal region (DG and CA3) was significantly increased in CLP, CLP + SF, and CLP + NLRP3 inhibitor groups, which all showed irregular cell borders, disorganized cell arrangement, and dark staining of the cytoplasm. Among them, the CLP group was especially obvious (Figure 2A). Moreover, Tunel staining (red signals) showed a significant increase in apoptosis in the hippocampal region (DG and CA3) and peripheral regions in CLP, CLP + SF and CLP + NLRP3 inhibitor groups than Control group. Among them, the CLP group was particularly obvious (Figure 2B and C).

Levels of the Inflammatory Cytokines IL-1β and IL-18 and the Inflammasomes NLRP3 and Caspase 1

In addition, inflammatory cytokines IL-1β and IL-18 levels in serum and brain tissues of mice showed that IL-1β and IL-18 levels were observably elevated in CLP group than Control group. IL-1β and IL-18 levels were reduced after treatment with SF and NLRP3 inhibitor respectively (Figure 3A–D). Furthermore, compared to Control group, NLRP3

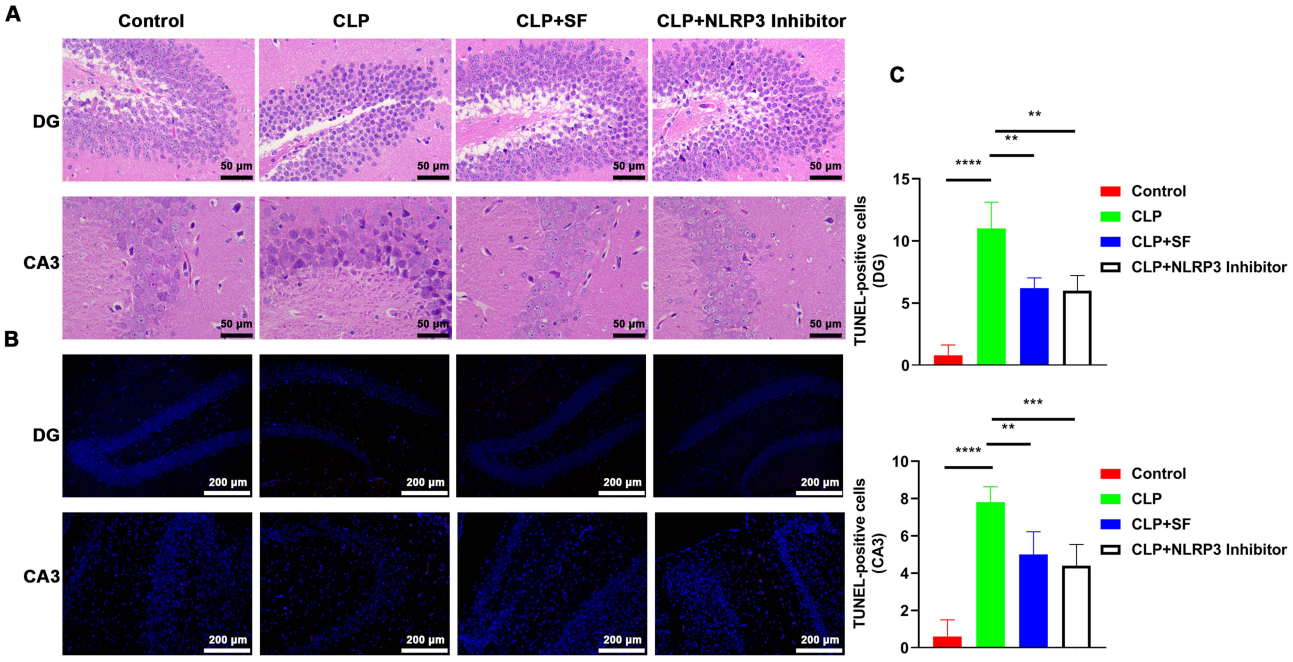

Figure 2 Pathological analysis of the hippocampal region of mouse brain tissue. (**A**) Hematoxylin-eosin staining was performed to observe the pathological changes of hippocampus (DG and CA3). Scale bar: 50 μm. (**B**) TdT mediated dUTP Nick End Labeling (Tunel) was utilized to evaluate apoptosis in hippocampus (DG and CA3) of brain tissueS. Red indicated Tunel signals, blue indicated the DAPI signals. Scale bar: 200 μm. (**C**) Statistical analysis of Tunel-positive cells. **P < 0.01; ***P < 0.001; ****P < 0.0001.
Abbreviations: CLP, caecal ligation and puncture; SF, shenfu injection.

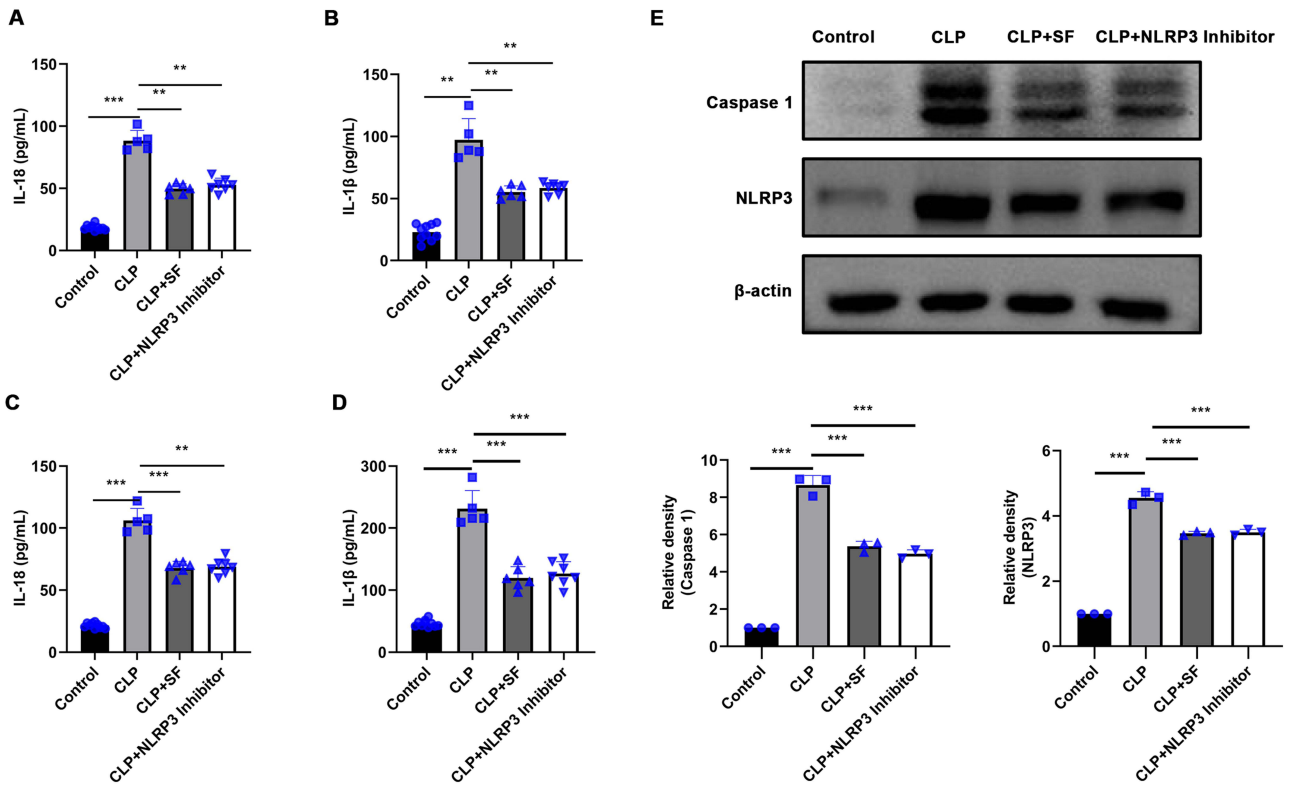

Figure 3 Levels of the inflammatory cytokines IL-1β and IL-18 and the inflammasomes NLRP3 and Caspase 1. (**A** and **B**) Enzyme-linked immunosorbent assay was applied to detect serum IL-1β and IL-18 levels. (**C** and **D**) Enzyme-linked immunosorbent assay was utilized to detect IL-1β and IL-18 levels in brain tissues. (**E**) Western blot analysis of NLRP3 and Caspase 1 expression in brain tissues. **P < 0.01, ***P < 0.001.

Abbreviations: CLP, caecal ligation and puncture; SF, shenfu injection; IL, interleukin; NLRP3, nucleotide binding oligomerization domain-like receptor family pyrin domain protein 3.

and Caspase 1 expressions in the brain tissues of CLP group were notably elevated. NLRP3 and Caspase 1 expressions were repressed after treatment with SF and NLRP3 inhibitor respectively (Figure 3E).

Expression of NLRP3/Caspase 1 and NeuN in Hippocampus of Brain Tissues

In addition, we further used IF staining to detect NLRP3/Caspase 1 and NeuN expression in hippocampus (DG and CA3) of brain tissues. The green fluorescence is NLRP3 or Caspase 1, the red fluorescence is NeuN, and the blue fluorescence is DAPI. Compared to Control group, the expression of NLRP3/Caspase 1 and NeuN in hippocampal neurons in CLP group was up-regulated. After treatment with SF and NLRP3 inhibitor respectively, the expression of NLRP3/Caspase 1 and NeuN in hippocampal neurons was decreased (Figure 4A–D).

The Acquisition of Active Ingredients of SF and the Molecular Docking Analysis of the Active Ingredients of SF and the Targets NLRP3 and Caspase 1

Next, we conducted a network pharmacological analysis. According to DL ≥ 0.18 and OB ≥ 30%, there were 43 active ingredients in SF. Among them, 22 were Renshen and 21 were Fuzi (Table 1). Cytoscape 3.7.0 was utilized to visualize the interaction between the active components of SF and the targets NLRP3 and Caspase 1, and to construct the compound-ingredient-target diagram. As shown in Figure 5A, the main active components of SF formed a complex regulatory network with NLRP3 and Caspase 1, indicating that TCM compounds were regulated through the synergistic action of multiple components and targets in regulating and restoring the balance of human function. In addition, in order to study the interaction between the active ingredients of SF and the targets NLRP3 and Caspase 1, TCMSP database was acted as the ligand library, and the PDB file obtained by the targets NLRP3 and Caspase 1 was used as the receptor protein, and the molecular docking was performed using Auto Dock Vina1.1.2. The binding energy ≤ −5.0 kJ·mol^{-1} was selected as the screening condition to obtain SF ingredients and targets NLRP3 and Caspase 1. Among them, 27

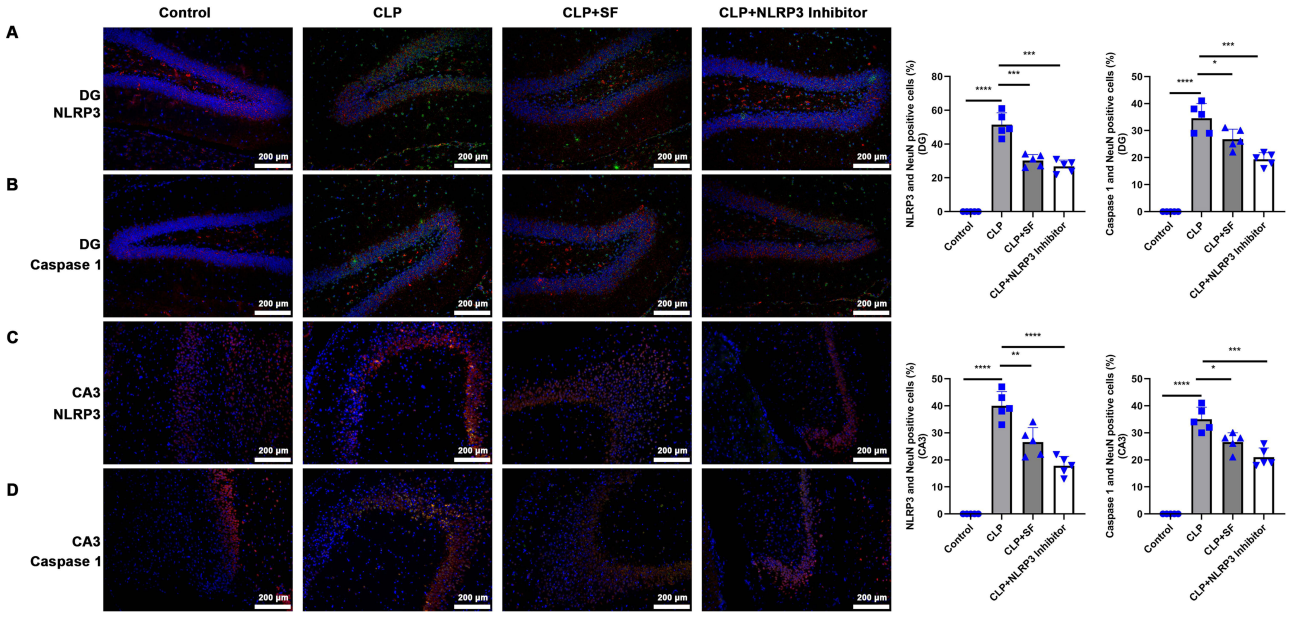

Figure 4 Expression of NLRP3/Caspase 1 and NeuN in hippocampus of mouse brain tissue. (**A**) NLRP3 and NeuN expressions in hippocampus (DG) was assessed by immunofluorescence staining. The green fluorescence is NLRP3, the red fluorescence is NeuN, and the blue fluorescence is DAPI. Scale bar: 200 μm. (**B**) Caspase 1 and NeuN expressions in hippocampus (DG) was measured by immunofluorescence staining. The green fluorescence is Caspase 1, the red fluorescence is NeuN, and the blue fluorescence is DAPI. Scale bar: 200 μm. (**C**) NLRP3 and NeuN expressions in hippocampus (CA3) was assessed by immunofluorescence staining. The green fluorescence is NLRP3, the red fluorescence is NeuN, and the blue fluorescence is DAPI. Scale bar: 200 μm. (**D**) Caspase 1 and NeuN expressions in hippocampus (CA3) was measured by immunofluorescence staining. The green fluorescence is Caspase 1, the red fluorescence is NeuN, and the blue fluorescence is DAPI. Scale bar: 200 μm. *P < 0.05, **P < 0.01, ***P < 0.001; ****P < 0.0001.

Abbreviations: CLP, caecal ligation and puncture; SF, shenfu injection; NLRP3, nucleotide binding oligomerization domain-like receptor family pyrin domain protein 3.

molecules were well bound to the target NLRP3, and 42 molecules were well bound to the target Caspase 1 (Table 2). The top three molecules with the closest binding degree to each target were selected to draw two- and three-dimensional graph using Discovery Studio 2019 software. Results showed in Supplemental Figure 1. In addition, PyMOL 2.5.4 was applied to visualize the molecular docking results. Results showed that (R)-norcoclaurine (MOL002419) was most closely bound to NLRP3 with binding energy of −7.2 kJ·mol^{-1}, ignavine (MOL002421) was most closely bound to Caspase 1 with binding energy of −8.3 kJ·mol^{-1} (Figure 5B and C, Table 2).

Table 1 Active Ingredient of Shenfu

Mol ID	OB (%)	DL	Herb
MOL002879	43.59	0.39	Renshen
MOL000449	43.83	0.76	Renshen
MOL000358	36.91	0.75	Renshen
MOL003648	65.83	0.54	Renshen
MOL000422	41.88	0.24	Renshen
MOL004492	38.72	0.58	Renshen
MOL005308	66.65	0.22	Renshen
MOL005314	101.88	0.49	Renshen
MOL005317	39.27	0.81	Renshen
MOL005318	40.45	0.2	Renshen
MOL005320	45.57	0.2	Renshen
MOL005321	65.9	0.34	Renshen
MOL005344	36.32	0.56	Renshen

(*Continued*)

Table 1 (Continued).

Mol ID	OB (%)	DL	Herb
MOL005348	31.11	0.78	Renshen
MOL005356	61.22	0.31	Renshen
MOL005357	31.99	0.83	Renshen
MOL005360	57.71	0.63	Renshen
MOL005376	33.09	0.79	Renshen
MOL005384	57.52	0.56	Renshen
MOL005399	36.91	0.75	Renshen
MOL005401	39.56	0.79	Renshen
MOL000787	59.26	0.83	Renshen
MOL002211	39.99	0.2	Fuzi
MOL002388	57.76	0.28	Fuzi
MOL002392	46.69	0.37	Fuzi
MOL002393	34.52	0.18	Fuzi
MOL002394	34.52	0.18	Fuzi
MOL002395	56.3	0.31	Fuzi
MOL002397	51.73	0.73	Fuzi
MOL002398	69.56	0.34	Fuzi
MOL002401	43.1	0.85	Fuzi
MOL002406	39.43	0.38	Fuzi
MOL002410	34.06	0.53	Fuzi
MOL002415	51.87	0.66	Fuzi
MOL002416	30.96	0.24	Fuzi
MOL002419	82.54	0.21	Fuzi
MOL002421	84.08	0.25	Fuzi
MOL002422	50.82	0.73	Fuzi
MOL002423	33.41	0.19	Fuzi
MOL002433	41.52	0.22	Fuzi
MOL002434	38.16	0.8	Fuzi
MOL000359	36.91	0.75	Fuzi
MOL000538	31.39	0.26	Fuzi

Abbreviations: DL, drug-likeness; OB, oral bioavailability.

Norcoclaurine Increases the Cell Viability and Decreases Inflammation and Apoptosis

Furthermore, BV-2 cells were treated with LPS was considered the in vitro model. Figure 6A showed that LPS decreased the cell viability compared to the Control group; while norcoclaurine, not DMSO (solvent of norcoclaurine) promoted the cell viability when compared to the LPS group. The expression levels of apoptosis related protein Caspase 1, inflammation related protein (NLRP3, IL-18, and IL-1β) were promoted by LPS treatment, while norcoclaurine, not DMSO, reduced the above protein upregulation induced by LPS (Figure 6B and C).

Discussion

Sepsis evoked systemic inflammation, including neuroinflammation.[28] SAE is a form of diffuse central nervous system dysfunction during sepsis, which is associated with increased mortality and poor prognosis in patients with sepsis.[29] Patients with SAE can present with a wide range of severity, ranging from mild delirium to deep coma. This condition is known to occur in up to 70% of patients in intensive care units.[30] Despite extensive research, specific treatments for SAE are still lacking.[31] In this study, we conducted in vivo experiments to investigate the specific mechanism of SF in SAE, which involved NLRP3/Caspase 1 mediated pyroptosis pathway. We found that SF reduced sepsis induced cognitive dysfunction by improving pyroptosis. This is the first time to report the study of SF/NLRP3/Caspase 1 mediated pyroptosis in SAE.

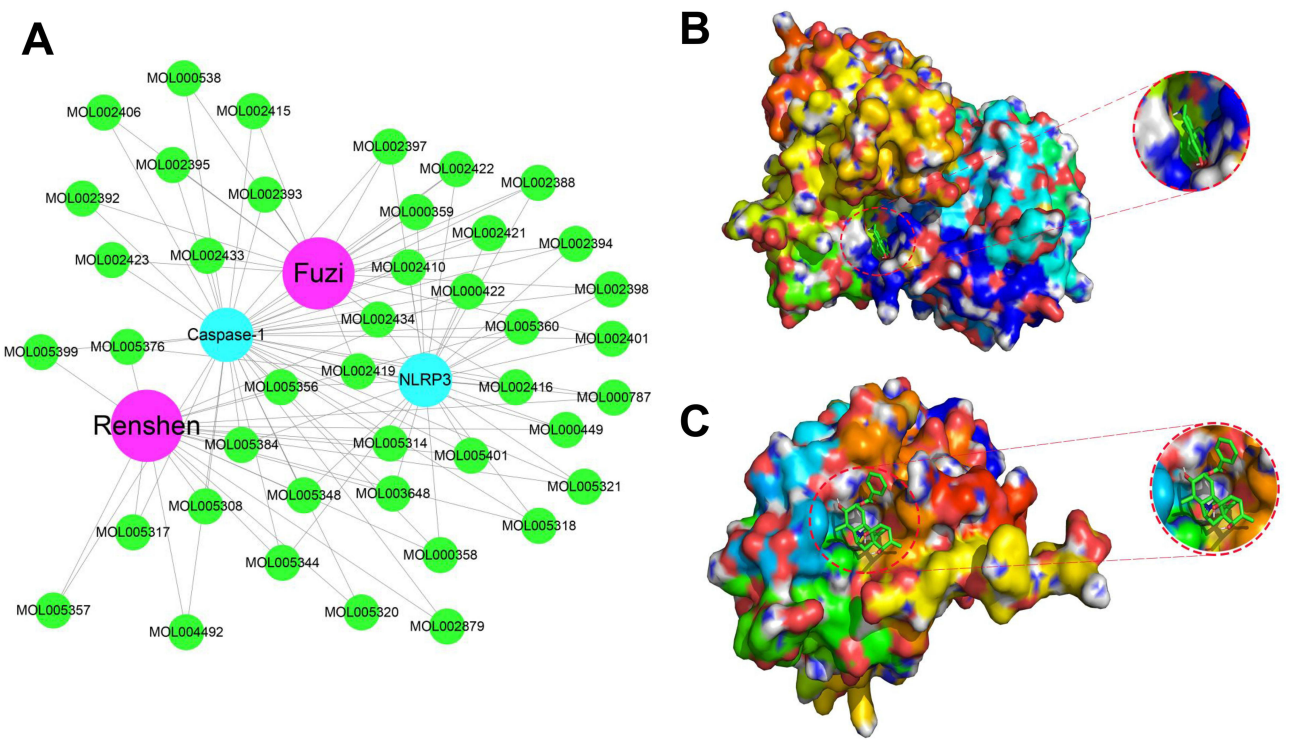

Figure 5 The acquisition of active ingredients of shenfu injection and the molecular docking analysis of the active ingredients of shenfu injection and the targets NLRP3 and Caspase 1. (**A**) Cytoscape3.7.0 was applied to visualize the interaction between the active components of shenfu injection and the targets NLRP3 and Caspase 1, and to construct the compound-ingredient-target diagram. (**B** and **C**) PyMOL 2.5.4 was utilized to visualize the molecular docking results of (R)-norcoclaurine with NLRP3 (**B**) and ignavine with Caspase 1 (**C**). NLRP3, nucleotide binding oligomerization domain-like receptor family pyrin domain protein 3.

As a Chinese medicinal preparation, SF is widely used in treating various diseases, including sepsis. Previous study has demonstrated that SF dose-dependently prolonged survival and protected intestinal mucosa in septic rats.[12] Xu et al reported that SF prevented sepsis-induced myocardial injury by inhibiting mitochondrial apoptosis.[32] In addition, SF has shown good clinical efficacy in treating sepsis.[33] However, the therapeutic effect of SF on SAE remains unclear. The use of CLP has been reported to induce experimental sepsis in mice, causing polymicrobial sepsis.[34] Polymicrobial sepsis caused by CLP is the most commonly employed model l due to its close resemblance to the progression and

Table 2 Molecular Docking Results of NLRP3 and Caspase 1 with the Active Ingredient of Shenfu

Mol ID	Target	PDB ID	Affinity/kJ mol-1
MOL002419	NLRP3	7ALV	−7.2
MOL003648	NLRP3	7ALV	−7
MOL005321	NLRP3	7ALV	−6.7
MOL005376	NLRP3	7ALV	−6.6
MOL000787	NLRP3	7ALV	−6
MOL005314	NLRP3	7ALV	−6
MOL002398	NLRP3	7ALV	−5.8
MOL002401	NLRP3	7ALV	−5.7
MOL005356	NLRP3	7ALV	−5.7
MOL000358	NLRP3	7ALV	−5.5
MOL000359	NLRP3	7ALV	−5.5
MOL002421	NLRP3	7ALV	−5.5

(*Continued*)

Table 2 (Continued).

Mol ID	Target	PDB ID	Affinity/kJ mol-1
MOL005348	NLRP3	7ALV	−5.5
MOL005401	NLRP3	7ALV	−5.5
MOL000449	NLRP3	7ALV	−5.4
MOL002434	NLRP3	7ALV	−5.3
MOL002388	NLRP3	7ALV	−5.2
MOL005344	NLRP3	7ALV	−5.2
MOL000422	NLRP3	7ALV	−5.1
MOL002410	NLRP3	7ALV	−5.1
MOL002422	NLRP3	7ALV	−5.1
MOL002394	NLRP3	7ALV	−5
MOL002397	NLRP3	7ALV	−5
MOL002416	NLRP3	7ALV	−5
MOL005318	NLRP3	7ALV	−5
MOL005360	NLRP3	7ALV	−5
MOL005384	NLRP3	7ALV	−5
MOL002421	Caspase-1	1BMQ	−8.3
MOL004492	Caspase-1	1BMQ	−8.2
MOL002410	Caspase-1	1BMQ	−7.7
MOL002401	Caspase-1	1BMQ	−7.6
MOL000787	Caspase-1	1BMQ	−7.5
MOL000538	Caspase-1	1BMQ	−7.1
MOL002392	Caspase-1	1BMQ	−7.1
MOL003648	Caspase-1	1BMQ	−7.1
MOL005344	Caspase-1	1BMQ	−7.1
MOL002433	Caspase-1	1BMQ	−7
MOL002434	Caspase-1	1BMQ	−7
MOL005357	Caspase-1	1BMQ	−7
MOL005384	Caspase-1	1BMQ	−7
MOL000422	Caspase-1	1BMQ	−6.9
MOL005318	Caspase-1	1BMQ	−6.9
MOL005376	Caspase-1	1BMQ	−6.9
MOL000358	Caspase-1	1BMQ	−6.8
MOL005321	Caspase-1	1BMQ	−6.8
MOL005356	Caspase-1	1BMQ	−6.8
MOL005401	Caspase-1	1BMQ	−6.8
MOL002398	Caspase-1	1BMQ	−6.7
MOL005314	Caspase-1	1BMQ	−6.7
MOL000449	Caspase-1	1BMQ	−6.6
MOL005348	Caspase-1	1BMQ	−6.6
MOL002395	Caspase-1	1BMQ	−6.5
MOL005360	Caspase-1	1BMQ	−6.5
MOL000359	Caspase-1	1BMQ	−6.4
MOL002388	Caspase-1	1BMQ	−6.4
MOL002393	Caspase-1	1BMQ	−6.4
MOL002419	Caspase-1	1BMQ	−6.4
MOL002394	Caspase-1	1BMQ	−6.3
MOL002415	Caspase-1	1BMQ	−6.2
MOL002416	Caspase-1	1BMQ	−6.2
MOL005399	Caspase-1	1BMQ	−6.2
MOL002397	Caspase-1	1BMQ	−6.1

(*Continued*)

Table 2 (Continued).

Mol ID	Target	PDB ID	Affinity/kJ mol-1
MOL002422	Caspase-1	1BMQ	−6.1
MOL005308	Caspase-1	1BMQ	−6.1
MOL005317	Caspase-1	1BMQ	−6.1
MOL002406	Caspase-1	1BMQ	−5.9
MOL002423	Caspase-1	1BMQ	−5.9
MOL002879	Caspase-1	1BMQ	−5.4
MOL005320	Caspase-1	1BMQ	−5.1

characteristics of human sepsis.[35] In addition, CLP-induced cognitive impairment.[36] In this study, we successfully constructed a mouse sepsis model with cognitive impairment through CLP method. Same with previous study,[36] the survival rate of CLP group decreased significantly. In addition, we found that the escape latency time increased

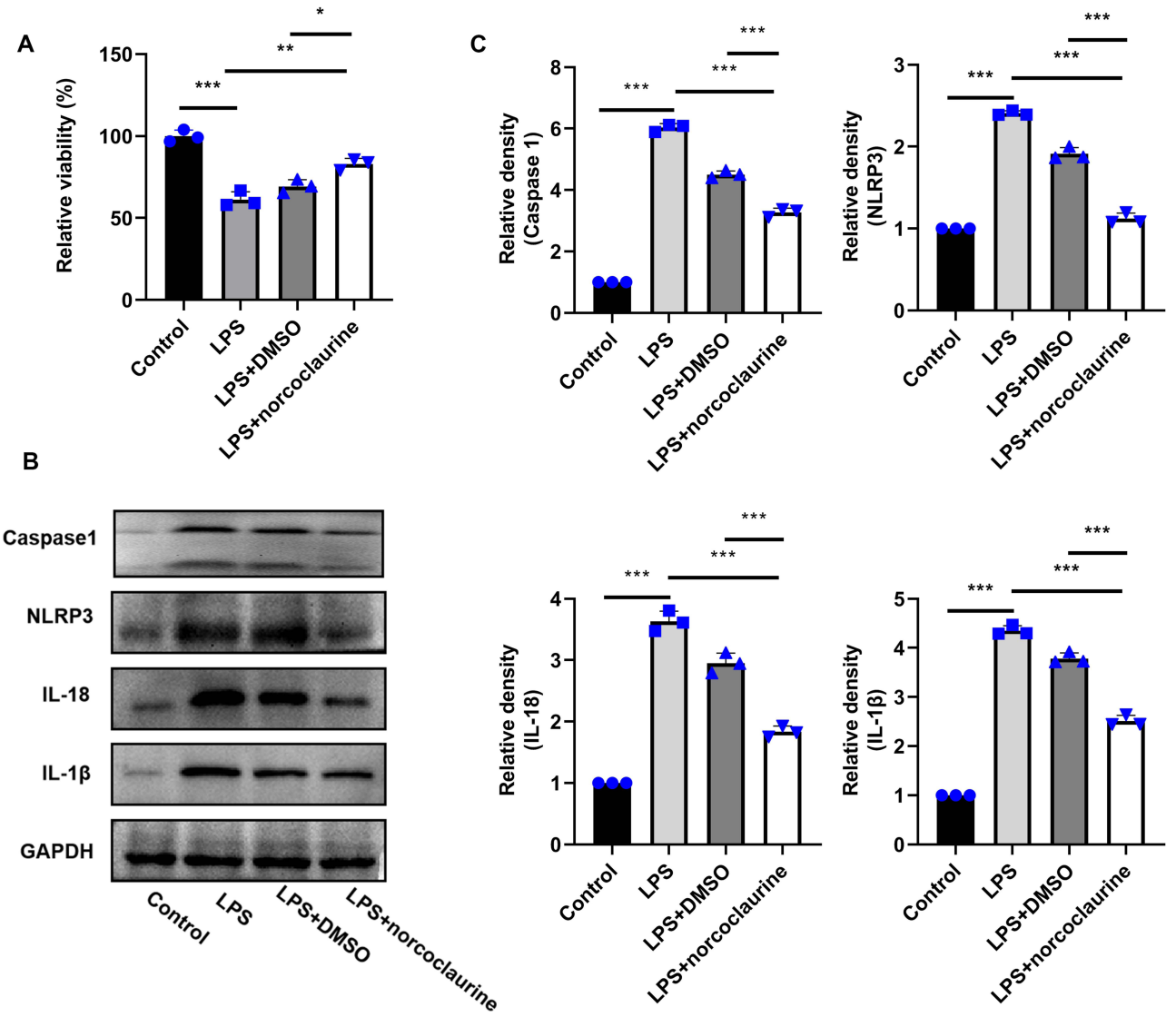

Figure 6 Norcoclaurine increases the cell viability and decreases inflammation and apoptosis. BV-2 cells were treated with/without LPS/norcoclaurine for 24 h. (**A**) Cell viability detection using Cell Counting Kit-8. (**B**) Western blot analysis of Caspase 1, NLRP3, IL-18, and IL-1β levels. (**C**) The relative density analysis of (**B**). *P < 0.05, **P < 0.01, ***P < 0.001.

Abbreviations: IL, interleukin; LPS, lipopolysaccharide; DMSO, dimethyl sulfoxide; NLRP3, nucleotide binding oligomerization domain-like receptor family pyrin domain protein 3.

significantly, and the number of crossings the platform decreased significantly. SF and NLRP3 inhibitor increased the survival rate of mice, decreased the escape latency time of mice. Hippocampus play key role in learning contextual information.[37] We found that neuronal damage and cell apoptosis in hippocampal region increased in CLP group. SF and NLRP3 inhibitor could improve neuronal damage and apoptosis in hippocampus region. These results indicated that SF could effectively alleviate SAE in mice. Therefore, we further explored the mechanism of SF in SAE in mice.

Pyroptosis plays an important role in host defense against pathogenic infections, and this process is planned by inflammasomes.[38] Activation of NLRP3 triggers the assembly of intracytoplasmic multiprotein signaling complexes, known as inflammasomes, which serve as platforms for the activation of Caspase 1. This activation, in turn, leads to the release of pro-inflammatory cytokines like IL-1β and IL-18, as well as cell death mediated by GSDMD.[39] The study results of Fu et al showed that hippocampal dependent memory deficit induced by CLP was accompanied by an increase in NLRP3 and Caspase 1 positive cells and an increase in protein levels of NLRP3, Caspase 1 and pro-inflammatory cytokines in the hippocampus.[19] Therefore, inhibition of pyroptosis may have potential therapeutic effects on SAE.[40] Sun et al reported that in juvenile rats with sepsis, P2X7 receptor-mediated NLRP3/Caspase 1-related pyroptosis occurs in the cerebral cortex through the ERK1/2 signaling pathway and plays a neuroprotective role.[41] In this study, we found that SF reduced inflammatory cytokines IL-1β and IL-18 levels in serum and brain tissue. In addition, SF could reduce the levels of inflammasome NLRP3 and Caspase 1 in brain and NLRP3/Caspase 1 and NeuN expressions in hippocampal neurons. Therefore, targeting NLRP3/Caspase 1-mediated pyroptosis may be a viable treatment for SAE.

Network pharmacology provides a new paradigm for uncovering and visualizing the potential interaction networks of TCM against multifactorial diseases.[42] Through collaborative multi-compound network pharmacology and drug reuse, precise and effective therapeutic interventions could be achieved, avoiding the need for drug discovery and accelerating clinical transformation.[43] Yuan et al employed a novel research approach using network pharmacology to identify potential therapeutic targets and key active ingredients of SF for sepsis based on the pathophysiological perspective of the condition. Through their analysis, they identified 28 active ingredients of SF, including 18 ginsenosides and 10 aconite alkaloids.[44] We found 43 active ingredients in SF through network pharmacological analysis, including 22 Renshen and 21 Fuzi. In addition, we found Renshen and Fuzi, the main active ingredients of SF, form a complex regulatory network with NLRP3 and Caspase 1. Study has indicated that the main bioactive ingredients of Fuzi-Gancao herb couple in the treatment of non-alcoholic fatty liver disease including (R)-norcoclaurine.[45] In addition, norcoclaurine significantly improve memory in Alzheimer's disease.[46] Ignavine is a novel allosteric modulator of the mu opioid receptors, which may be used to treat pain.[47] However, the relationship between (R)-norcoclaurine/ignavine and NLRP3/Caspase 1 in SAE is unclear. Through molecular docking, we found that (R)-norcoclaurine (MOL002419) was most closely bound to NLRP3 with binding energy of −7.2 $kJ \cdot mol^{-1}$, ignavine (MOL002421) was most closely bound to Caspase 1 with binding energy of −8.3 $kJ \cdot mol^{-1}$. These results suggested that SF might improve SAE by modulating NLRP3/Caspase 1 via (R)-norcoclaurine and ignavine. In addition, we found that norcoclaurine increased the cell viability and decreased inflammation and apoptosis. Therefore, we speculated that norcoclaurine could prevent SAE. Furthermore, we will further validate the preventive effects of norcoclaurine and ignavine on SAE in animal experiments.

Conclusion

Our results suggested that SF could improve SAE, which may be involved in NLRP3/Caspase 1 mediated pyroptosis. Moreover, SF could regulate NLRP3/Caspase 1 through (R)-norcoclaurinee to prevent SAE. Therefore, our study provides clues to understand the molecular mechanism of SF in SAE, and provides a new idea for treating SAE.

Abbreviation

SAE, sepsis-associated encephalopathy; SF, shenfu injection; CLP, caecal ligation and puncture; MWM, Morris water maze; TCM, traditional Chinese medicine; NLRP3, nucleotide binding oligomerization domain-like receptor family pyrin domain protein 3; HE, hematoxylin-eosin; Tunel, TdT mediated dUTP Nick End Labeling; ELISA, enzyme-linked immunosorbent assay; IF, immunofluorescence; GSDMD, gasdermin D; PBS, phosphate buffer saline; IL, interleukin; LPS, lipopolysaccharide; DMSO, dimethyl sulfoxide; CCK-8, Cell Counting Kit-8.

Data Sharing Statement

The datasets generated during and/or analyzed during the current study showed in the manuscript.

Ethic Statements

All animal experiments have been approved by ethics committee of Guangdong Provincial People's Hospital (approval number KY–H–2022-004-03), and performed in according with the IACUC Handbook, Third Edition.

Author Contributions

All authors made a significant contribution to the work reported, whether that is in the conception, study design, execution, acquisition of data, analysis and interpretation, or in all these areas; took part in drafting, revising or critically reviewing the article; gave final approval of the version to be published; have agreed on the journal to which the article has been submitted; and agree to be accountable for all aspects of the work.

Funding

This work was supported by the [Science and Technology Program of Guangzhou] (grant number [202102080123]), the [Scientific research project of Guangdong traditional Chinese Medicine Bureau] (grant number [20211009]), the [Wu Jieping Medical Foundation Runze Fund for Critical Care Medicine] (grant number [320.6750.2022-02-9]), and the [Guangdong Provincial People's Hospital Interior Project] (grant numbers [8207081293], [8217080600], and [8237080084]).

Disclosure

The authors have no relevant financial or non-financial interests to disclose.

References

1. Wang J, Yang S, Jing G, et al. Inhibition of ferroptosis protects sepsis-associated encephalopathy. *Cytokine*. 2023;161:156078. doi:10.1016/j.cyto.2022.156078
2. Krzyzaniak K, Krion R, Szymczyk A, Stepniewska E, Sieminski M. Exploring neuroprotective agents for sepsis-associated encephalopathy: a comprehensive review. *Int J Mol Sci*. 2023;24(13). doi:10.3390/ijms241310780
3. Dumbuya JS, Li S, Liang L, Zeng Q. Paediatric sepsis-associated encephalopathy (SAE): a comprehensive review. *Mol Med*. 2023;29(1):27. doi:10.1186/s10020-023-00621-w
4. Gao S, Jiang Y, Chen Z, et al. Metabolic reprogramming of microglia in sepsis-associated encephalopathy: insights from neuroinflammation. *Curr Neuropharmacol*. 2023;21(9):1992–2005. doi:10.2174/1570159x21666221216162606
5. Liu Y, Yang H, Luo N, et al. An Fgr kinase inhibitor attenuates sepsis-associated encephalopathy by ameliorating mitochondrial dysfunction, oxidative stress, and neuroinflammation via the SIRT1/PGC-1α signaling pathway. *J Transl Med*. 2023;21(1):486. doi:10.1186/s12967-023-04345-7
6. Song Y, Zhang N, Shi S, et al. Large-scale qualitative and quantitative characterization of components in Shenfu injection by integrating hydrophilic interaction chromatography, reversed phase liquid chromatography, and tandem mass spectrometry. *J Chromatogr A*. 2015;1407:106–118. doi:10.1016/j.chroma.2015.06.041
7. Xiao L, Niu L, Xu X, et al. Comparative efficacy of tonic Chinese herbal injections for treating sepsis or septic shock: a systematic review and bayesian network meta-analysis of randomized controlled trials. *Front Pharmacol*. 2022;13:830030. doi:10.3389/fphar.2022.830030
8. Li X, Huang F, Zhu L, et al. Effects of combination therapy with Shenfu Injection in critically ill patients with septic shock receiving mechanical ventilation: a multicentric, real-world study. *Front Pharmacol*. 2022;13:1041326. doi:10.3389/fphar.2022.1041326
9. Yang H, Liu L, Gao W, Liu K, Qi LW, Li P. Direct and comprehensive analysis of ginsenosides and diterpene alkaloids in Shenfu injection by combinatory liquid chromatography-mass spectrometric techniques. *J Pharm Biomed Anal*. 2014;92:13–21. doi:10.1016/j.jpba.2013.12.041
10. Li P, Lv B, Jiang X, et al. Identification of NF-κB inhibitors following Shenfu injection and bioactivity-integrated UPLC/Q-TOF-MS and screening for related anti-inflammatory targets in vitro and in silico. *J Ethnopharmacol*. 2016;194:658–667. doi:10.1016/j.jep.2016.10.052
11. Fen-fang H, Fa-xian G, Ying Z, et al. Shenfu injection protects human ECV304 cells from hydrogen peroxide via its anti-apoptosis way. *J Ethnopharmacol*. 2015;163:203–209. doi:10.1016/j.jep.2015.01.032
12. Jin S, Jiang R, Lei S, et al. Shenfu injection prolongs survival and protects the intestinal mucosa in rats with sepsis by modulating immune response. *Turk J Gastroenterol*. 2019;30(4):364–371. doi:10.5152/tjg.2019.18418
13. Zhao L, Jin L, Luo Y, et al. Shenfu injection attenuates cardiac dysfunction and inhibits apoptosis in septic mice. *Ann Transl Med*. 2022;10(10):597. doi:10.21037/atm-22-836
14. Zhang N, Liu J, Qiu Z, Ye Y, Zhang J, Lou T. Shenfu injection for improving cellular immunity and clinical outcome in patients with sepsis or septic shock. *Am J Emerg Med*. 2017;35(1):1–6. doi:10.1016/j.ajem.2016.09.008
15. Berkel C, Cacan E. Pollutant-induced pyroptosis in humans and other animals. *Life Sci*. 2023;316:121386. doi:10.1016/j.lfs.2023.121386
16. Zhang Y, Yang W, Li W, Zhao Y. NLRP3 Inflammasome: checkpoint Connecting Innate and Adaptive Immunity in Autoimmune Diseases. *Front Immunol*. 2021;12:732933. doi:10.3389/fimmu.2021.732933

17. Shi X, Tan S, Tan S. NLRP3 inflammasome in sepsis (Review). *Mol Med Rep*. 2021;24(1). doi:10.3892/mmr.2021.12153
18. Zhao S, Chen F, Yin Q, Wang D, Han W, Zhang Y. Reactive oxygen species interact with NLRP3 inflammasomes and are involved in the inflammation of sepsis: from mechanism to treatment of progression. *Front Physiol*. 2020;11:571810. doi:10.3389/fphys.2020.571810
19. Fu Q, Wu J, Zhou XY, et al. NLRP3/caspase-1 pathway-induced pyroptosis mediated cognitive deficits in a mouse model of sepsis-associated encephalopathy. *Inflammation*. 2019;42(1):306–318. doi:10.1007/s10753-018-0894-4
20. Zhou S, Li Y, Hong Y, Zhong Z, Zhao M. Puerarin protects against sepsis-associated encephalopathy by inhibiting NLRP3/Caspase-1/GSDMD pyroptosis pathway and reducing blood-brain barrier damage. *Eur J Pharmacol*. 2023;945:175616. doi:10.1016/j.ejphar.2023.175616
21. Li Y, Wang F, Luo Y. Ginsenoside Rg1 protects against sepsis-associated encephalopathy through beclin 1-independent autophagy in mice. *J Surg Res*. 2017;207:181–189. doi:10.1016/j.jss.2016.08.080
22. Li S, Guo Z, Zhang ZY. Protective effects of NLRP3 inhibitor MCC950 on sepsis-induced myocardial dysfunction. *J Biol Regul Homeost Agents*. 2021;35(1):141–150. doi:10.23812/20-662-a
23. Bai Y, Li L, Dong B, Ma W, Chen H, Yu Y. Phosphorylation-mediated PI3K-Art signalling pathway as a therapeutic mechanism in the hydrogen-induced alleviation of brain injury in septic mice. *J Cell Mol Med*. 2022;26(22):5713–5727. doi:10.1111/jcmm.17568
24. Zhao L, Song Y, Zhang Y, et al. HIF-1α/BNIP3L induced cognitive deficits in a mouse model of sepsis-associated encephalopathy. *Front Immunol*. 2022;13:1095427. doi:10.3389/fimmu.2022.1095427
25. Tang F, Chen L, Gao H, et al. Munc18-1 contributes to hippocampal injury in septic rats through regulation of Syntaxin1A and synaptophysin and glutamate levels. *Neurochem Res*. 2023;48(3):791–803. doi:10.1007/s11064-022-03806-7
26. Zhang Y, Chopp M, Meng Y, et al. Cerebrolysin improves cognitive performance in rats after mild traumatic brain injury. *J Neurosurg*. 2015;122 (4):843–855. doi:10.3171/2014.11.Jns14271
27. Wang H, Zhou XM, Wu LY, et al. Aucubin alleviates oxidative stress and inflammation via Nrf2-mediated signaling activity in experimental traumatic brain injury. *J Neuroinflammation*. 2020;17(1):188. doi:10.1186/s12974-020-01863-9
28. Guo Q, Gobbo D, Zhao N, et al. Adenosine triggers early astrocyte reactivity that provokes microglial responses and drives the pathogenesis of sepsis-associated encephalopathy in mice. *Nat Commun*. 2024;15(1):6340. doi:10.1038/s41467-024-50466-y
29. Gao YL, Liu YC, Zhang X, Shou ST, Chai YF. Insight into regulatory T cells in sepsis-associated encephalopathy. *Front Neurol*. 2022;13:830784. doi:10.3389/fneur.2022.830784
30. Yang K, Chen J, Wang T, Zhang Y. Pathogenesis of sepsis-associated encephalopathy: more than blood-brain barrier dysfunction. *Mol Biol Rep*. 2022;49(10):10091–10099. doi:10.1007/s11033-022-07592-x
31. Li Y, Fan Z, Jia Q, et al. Chaperone-mediated autophagy (CMA) alleviates cognitive impairment by reducing neuronal death in sepsis-associated encephalopathy (SAE). *Exp Neurol*. 2023;365:114417. doi:10.1016/j.expneurol.2023.114417
32. Xu P, Zhang WQ, Xie J, Wen YS, Zhang GX, Lu SQ. Shenfu injection prevents sepsis-induced myocardial injury by inhibiting mitochondrial apoptosis. *J Ethnopharmacol*. 2020;261:113068. doi:10.1016/j.jep.2020.113068
33. Xu C, Xia Y, Jia Z, Wang S, Zhao T, Wu L. The curative effect of Shenfu-injection in the treatment of burn sepsis and its effect on the patient's immune function, HMGB, and vWF. *Am J Transl Res*. 2022;14(4):2428–2435.
34. Siempos II, Lam HC, Ding Y, Choi ME, Choi AM, Ryter SW. Cecal ligation and puncture-induced sepsis as a model to study autophagy in mice. *J Vis Exp*. 2014;84:e51066. doi:10.3791/51066
35. Dejager L, Pinheiro I, Dejonckheere E, Libert C. Cecal ligation and puncture: the gold standard model for polymicrobial sepsis? *Trends Microbio*. 2011;19(4):198–208. doi:10.1016/j.tim.2011.01.001
36. Yin XY, Tang XH, Wang SX, et al. HMGB1 mediates synaptic loss and cognitive impairment in an animal model of sepsis-associated encephalopathy. *J Neuroinflammation*. 2023;20(1):69. doi:10.1186/s12974-023-02756-3
37. Smith DM, Mizumori SJ. Hippocampal place cells, context, and episodic memory. *Hippocampus*. 2006;16(9):716–729. doi:10.1002/hipo.20208
38. Cao Q, Zong J, Zhang Z, et al. Pyroptosis in fish research: a promising target for disease management. *Fish Shellfish Immunol*. 2023;139:108866. doi:10.1016/j.fsi.2023.108866
39. Wang L, Hauenstein AV. The NLRP3 inflammasome: mechanism of action, role in disease and therapies. *Mol Aspects Med*. 2020;76:100889. doi:10.1016/j.mam.2020.100889
40. Wang Y, Liu X, Wang Q, Yang X. Roles of the pyroptosis signaling pathway in a sepsis-associated encephalopathy cell model. *J Int Med Res*. 2020;48(8):300060520949767. doi:10.1177/0300060520949767
41. Sun X, Zhou R, Lei Y, Hu J, Li X. The ligand-gated ion channel P2X7 receptor mediates NLRP3/caspase-1-mediated pyroptosis in cerebral cortical neurons of juvenile rats with sepsis. *Brain Res*. 2020;1748:147109. doi:10.1016/j.brainres.2020.147109
42. Li X, Liu Z, Liao J, Chen Q, Lu X, Fan X. Network pharmacology approaches for research of Traditional Chinese Medicines. *Chin J Nat Med*. 2023;21(5):323–332. doi:10.1016/s1875-5364(23)60429-7
43. Nogales C, Mamdouh ZM, List M, Kiel C, Casas AI, Schmidt H. Network pharmacology: curing causal mechanisms instead of treating symptoms. *Trends Pharmacol Sci*. 2022;43(2):136–150. doi:10.1016/j.tips.2021.11.004
44. Yuan H, Liu Y, Huang K, Hao H, Xue YT. Therapeutic mechanism and key active ingredients of shenfu injection in sepsis: a network pharmacology and molecular docking approach. *Evid Based Complement Alternat Med*. 2022;2022:9686149. doi:10.1155/2022/9686149
45. Liu K, Xu Y, Zhang G, Xiang Z. Therapeutic effect and mechanism prediction of Fuzi-Gancao Herb couple on non-alcoholic fatty liver disease (NAFLD) based on network pharmacology and molecular docking. *Comb Chem High Throughput Screen*. 2023. doi:10.2174/1386207326666230614102412
46. Khan S, Khan HU, Khan FA, et al. Anti-Alzheimer and antioxidant effects of Nelumbo nucifera L. Alkaloids, Nuciferine and norcoclaurine in alloxan-induced diabetic albino rats. *Pharmaceuticals*. 2022;15(10):1205. doi:10.3390/ph15101205
47. Ohbuchi K, Miyagi C, Suzuki Y, et al. Ignavine: a novel allosteric modulator of the μ opioid receptor. *Sci Rep*. 2016;6:31748. doi:10.1038/srep31748